Efficient simulation of crack growth in multiple-crack systems considering internal boundaries and interfaces

Paul Judt[1,*], Andreas Ricoeur[1]

[1] Department of Engineering Mechanics, University of Kassel, 34125 Kassel, Germany
[*]Corresponding author: judt@uni-kassel.de

Abstract The paper presents numerical methods used for predicting crack paths in technical structures based on the theory of linear elastic fracture mechanics. To simulate crack growth, the FE-method is used in combination with a smart re-meshing algorithm. Different methods providing accurate crack loading parameters particularly for curved cracks such as the J-integral or stress intensity factors (SIF) are presented. Path-independent contour integrals [12] are used to avoid special requirements concerning crack tip meshing and to enable efficient calculations for domains including interfaces and internal boundaries. The integration paths being finite and far from the crack tip, special attention has to be directed to the treatment of the crack face integral since the calculation of the coordinate J_2 is challenging [5]. The same holds for the coordinate M_2^{II} of the interaction integral related to a mode-II auxiliary loading. In particular, the interaction of multiple cracks and internal boundaries and interfaces is investigated. Calculating the global J-integral, including all crack tips existing in a structure, leads to the necessity of a separation procedure to determine the parts of J related to each single crack tip.

Keywords J-integral, M-integral, mixed-mode fracture, curved crack faces, fictitious crack faces

1. Introduction

Path-independent integrals are widely applied to calculate loading quantities such as stress intensity factors, the energy release rate or the J-integral. The J-integral is based on Eshelby's [6] general theory of forces acting at singularities. Rice [12] and Cherepanov [4] applied the formulation of this path-independent integral to strain concentration problems like notches and cracks. Herrmann and Herrmann [10] extended Rices' approach of J, which was limited to straight cracks, by a formulation of the two-dimensional J_k-integral vector which is composed of the coordinate $J_1 = J$ and J_2. Bergez [2] presented a relation between J_k-integral and SIF. It is well-known that the calculation of the J_2-integral is challenging since the numerical treatment of the singular stresses at the crack tip is going along with problems finally leading to inaccurate results. A semi-analytical approach for the calculation of J_2 considering straight cracks was presented by Eischen [5].
The M-integral is a conservation integral based on the superposition of two loading scenarios [13, 14], i.e. the actual and an auxiliary loading. In general, the near tip solution is employed to obtain auxiliary fields limiting this method to straight cracks in homogeneous materials without interfaces. Gosz et. al. [7, 8] applied the M-integral to three-dimensional crack problems considering interfaces and curved crack fronts, however still maintaining straight crack faces.
This paper presents two new methods for calculating accurate values of J_2 which are valid for straight and curved cracks. Further, the M_k-interaction integral vector is calculated for arbitrary curved crack faces.
Crack path predictions for multiple crack systems are carried out classically by applying crack tip elements [3] or the M-integral associated with small integration contours [16]. Additionally, a separation procedure is introduced, to calculate accurate loading quantities from a global J_k-integral calculation, representing the sum of all $J_k^{(i)}$-integral vectors, related to the i-th crack tip. Resulting crack paths of a crack propagation simulation considering two cracks are presented.

2. Path-independent contour integrals

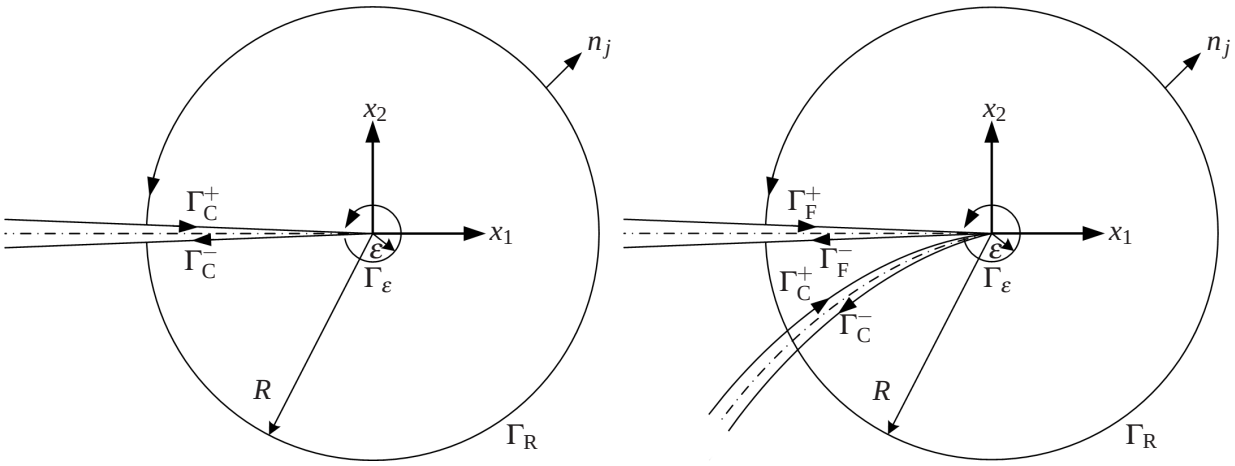

Figure 1. Integration contours, actual and fictitious crack faces Γ_C and Γ_F for path-independent J_k and M_k-integrals.

Within the theory of Linear Elastic Fracture Mechanics (LEFM) the J_k-integral vector is a path-independent energy conservation integral. With an integration contour Γ_ε in the vicinity of the crack tip at a distance ε, the J_k-integral is defined as

$$J_k = \lim_{\varepsilon \to 0} \int_{\Gamma_\varepsilon} Q_{kj} n_j \mathrm{d}s \tag{1}$$

with Eshelby's tensor Q_{kj}, including the stress tensor σ_{mn}, the strain tensor ε_{mn} and the displacement derivatives $u_{i,k}$:

$$Q_{kj} = \frac{1}{2}\sigma_{mn}\varepsilon_{mn}\delta_{kj} - \sigma_{ij}u_{i,k} \tag{2}$$

The Kronecker identity tensor is denoted as δ_{kj}. In LEFM the coordinates of Eq. (1) are related directly to the stress intensity factors [2]:

$$J_1 = \frac{K_\mathrm{I}^2 + K_\mathrm{II}^2}{E'}, \qquad J_2 = -2\frac{K_\mathrm{I} K_\mathrm{II}}{E'} \tag{3}$$

For plain stress $E' = E$ and for plain strain $E' = E/\left(1-\nu^2\right)$. The energy release rate G is the projection of J_k onto the unit vector of crack propagation direction z_k:

$$G = J_k z_k \tag{4}$$

If the J_k-integral is calculated, assuming two different superimposed loading scenarios $^{(1)}$ and $^{(2)}$ for an arbitrary crack configuration, one obtains the following expression:

$$J_k^{(1)+(2)} = \lim_{\varepsilon \to 0} \int_{\Gamma_\varepsilon} Q_{kj}^{(1)+(2)} n_j \mathrm{d}s = \lim_{\varepsilon \to 0} \int_{\Gamma_\varepsilon} \left(Q_{kj}^{(1)} + Q_{kj}^{(2)} + Q_{kj}^{(1/2)}\right) n_j \mathrm{d}s = J_k^{(1)} + J_k^{(2)} + J_k^{(1/2)} \tag{5}$$

The third term of Eq. (5) is the interaction integral vector $J_k^{(1/2)}$ and will be denoted from now on as M_k,

$$M_k = \lim_{\varepsilon \to 0} \int_{\Gamma_\varepsilon} Q_{kj}^{(1/2)} n_j \mathrm{d}s \tag{6}$$

with Eshelby's tensor related to the interaction integral

$$Q_{kj}^{(1/2)} = \frac{1}{2}\left(\sigma_{mn}^{(1)}\varepsilon_{mn}^{(2)} + \sigma_{mn}^{(2)}\varepsilon_{mn}^{(1)}\right)\delta_{kj} - \left(\sigma_{ij}^{(1)}u_{i,k}^{(2)} + \sigma_{ij}^{(2)}u_{i,k}^{(1)}\right) \tag{7}$$

For straight crack faces, the near-tip solution yields valid fields ε_{mn}, σ_{mn}, $u_{i,k}$ associated to an auxiliary loading configuration and is therefore usually applied as auxiliary field. The relation between the coordinates of Eq. (6) and stress intensity factors is as follows:

$$M_1^{\mathrm{I}} = 2\frac{K_{\mathrm{I}}}{E'}, \qquad M_2^{\mathrm{I}} = -2\frac{K_{\mathrm{II}}}{E'}, \qquad M_1^{\mathrm{II}} = 2\frac{K_{\mathrm{II}}}{E'}, \qquad M_2^{\mathrm{II}} = -2\frac{K_{\mathrm{I}}}{E'} \tag{8}$$

The superscripts I and II denote a single mode-I or single mode-II auxiliary loading. If finite integration contours Γ_{R} are considered, the coordinates of J_k and M_k in general become path-dependent. If crack faces are straight, see Fig. 1(a), the path-dependence is restricted to J_2 and M_2^{II} in the case of mixed-mode loading. If curved crack faces are considered, see Γ_{C} in Fig. 1(b), both coordinates of J_k and M_k are depending on the chosen integration contour Γ_R. To hold path-independence, crack face integrals with $\mathrm{d}\Gamma_{\mathrm{C}} = \mathrm{d}\Gamma_{\mathrm{C}}^{+} = -\mathrm{d}\Gamma_{\mathrm{C}}^{-}$ have to be introduced, describing the jump of Eshelby's tensor across the crack faces:

$$J_k = \int_{\Gamma_{\mathrm{R}}} Q_{kj} n_j \mathrm{d}s + \int_{\Gamma_{\mathrm{C}}} \left[\!\left[Q_{kj} \right]\!\right]_{-}^{+} n_j \mathrm{d}s \tag{9a}$$

$$M_k = \int_{\Gamma_{\mathrm{R}}} Q_{kj}^{(1/2)} n_j \mathrm{d}s + \int_{\Gamma_{\mathrm{C}}} \left[\!\left[Q_{kj}^{(1/2)} \right]\!\right]_{-}^{+} n_j \mathrm{d}s \tag{9b}$$

In contrast to the J_k-integral according to Eq. (9a), the M_k-integral according to Eq. (9b) is still not path-independent, if curved crack faces are considered. Path-independence is finally achieved including an integration along the fictitious crack surfaces $\mathrm{d}\Gamma_{\mathrm{F}} = \mathrm{d}\Gamma_{\mathrm{F}}^{+} = -\mathrm{d}\Gamma_{\mathrm{F}}^{-}$, see Fig. 1(b):

$$M_k = \int_{\Gamma_{\mathrm{R}}} Q_{kj}^{(1/2)} n_j \mathrm{d}s + \int_{\Gamma_{\mathrm{C}}} \left[\!\left[Q_{kj}^{(1/2)} \right]\!\right]_{-}^{+} n_j \mathrm{d}s + \int_{\Gamma_{\mathrm{F}}} \left[\!\left[Q_{kj}^{(1/2)} \right]\!\right]_{-}^{+} n_j \mathrm{d}s \tag{10}$$

These are corresponding to the auxiliary fields which are taken from the asymptotic crack tip solutions. Thus, the fictitious crack faces Γ_{F} and the actual ones Γ_{C} always coincide at the crack tip. The integration in the vicinity of the crack tip based on numerical values provided from the FE-calculation is challenging. As the numerical representation of the singularity in stresses and strains deviates strongly from analytic solutions, the calculation of crack face integrals needs a special treatment.

3. Extended crack face integration

In this section, two methods are presented producing sufficiently accurate results for the crack face integration. Both are applied to the J_k- and M_k- integral calculation, however only the first one is

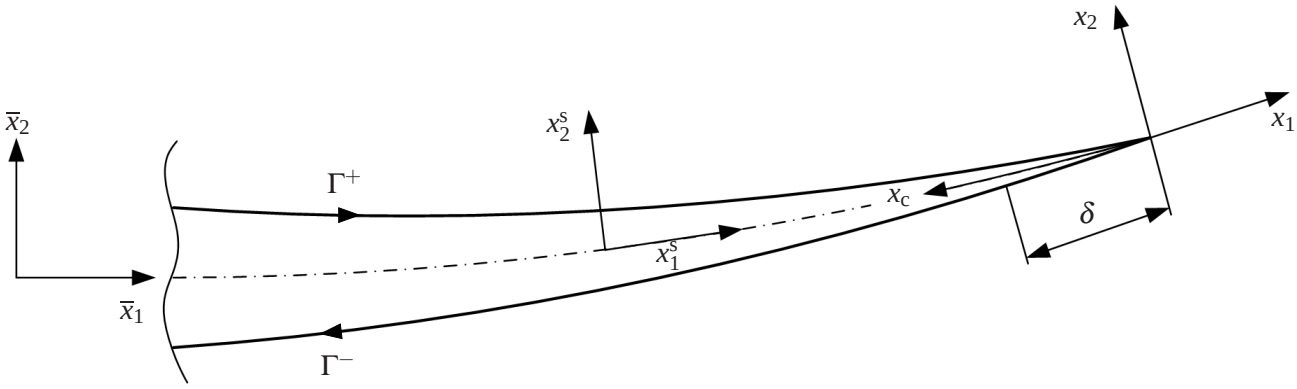

Figure 2. Curved crack faces Γ^+, Γ^-, crack tip coordinate system x_i, global coordinate system $\overline{x}_i$, local crack face coordinate system x_i^s depending on the position, arc length x_c along the crack faces with its origin at the crack tip, region δ where numerically calculated values for crack face integrals deviate strongly from the analytic ones.

presented here.
When calculating J_k by integrating along a circular contour Γ_R with the radius R and considering curved cracks as shown in Fig. 1(b), the crack face integral needs to be taken into account. Is the crack face integral calculated conventionally, this leads to a considerable error in the second coordinate J_2, and therefore in the SIF calculated from J_k with Eqs. (3):

$$K_{\mathrm{I}} = \pm\sqrt{\frac{E' J_1}{2}\left[1 \pm \sqrt{1-\left(\frac{J_2}{J_1}\right)^2}\right]}, \qquad K_{\mathrm{II}} = \pm\sqrt{\frac{E' J_1}{2}\left[1 \mp \sqrt{1-\left(\frac{J_2}{J_1}\right)^2}\right]} \tag{11}$$

3.1. Method 1: Analytic extension method

In the vicinity of the crack tip, the integrand can be formulated analytically. Therefore, the crack face integral of Eq. (9a) is divided into one part calculated numerically and the other part calculated analytically:

$$J_k = \int_{\Gamma_{\mathrm{R}}} Q_{kj} n_j \mathrm{d}s + \int_{R}^{\delta} \left[\!\left[Q_{kj} \right]\!\right]_{-}^{+} n_j \mathrm{d}s + \int_{\delta}^{0} \left[\!\left[Q_{kj} \right]\!\right]_{-}^{+} n_j \mathrm{d}s \tag{12}$$

The parameter δ separates both parts, see Fig. 2. The crack is assumed to be straight in the vicinity of the crack tip, as the curvature can be neglected for small δ. For such a crack, the dominant terms are the first terms of the series expansions $\sigma_{ij}^{(n)}$ and $u_i^{(n)}$ found by Williams [15], representing an infinite sum of eigenfunctions, completely describing the stress and displacement fields in a cracked body

$$\sigma_{ij}^{(n)}(r,\varphi) = \sum_{n=1}^{\infty} r^{\frac{n}{2}-1}\left[a_n M_{ij}^{(n)}(\varphi) + b_n N_{ij}^{(n)}(\varphi)\right] \tag{13a}$$

$$u_i^{(n)}(r,\varphi) = \frac{1}{2\mu}\sum_{n=1}^{\infty} r^{\frac{n}{2}}\left[a_n F_i^{(n)}(\varphi) + b_n G_i^{(n)}(\varphi)\right] \tag{13b}$$

with a_n and b_n being constant coefficients and $M_{ij}^{(n)}(\varphi)$, $N_{ij}^{(n)}(\varphi)$, $F_i^{(n)}(\varphi)$ and $G_i^{(n)}(\varphi)$ trigonometric angular functions. The coefficients a_1 and b_1 of the first eigenfunction are related to the SIF K_I and K_II and the coefficient a_2 of the second eigenfunction is related to the T-stress T_{11}:

$$K_\mathrm{I} - \mathrm{i}K_\mathrm{II} = \sqrt{2\pi}\,(a_1 + \mathrm{i}b_1)\,, \qquad T_{11} = 4a_2 \tag{14}$$

Substituting Eqs. (13) into Eq. (2), calculating the jump of Eshelby's tensor across the crack faces according to the third term on the right hand side of Eq. (12) and considering Eq. (14), the analytical part of the crack face integral is obtained:

$$J_2^\mathrm{ana} = \int_\delta^0 \left[\!\left[Q_{kj} \right]\!\right]_-^+ \mathrm{d}s = 8\,\frac{K_\mathrm{II} T_{11}\sqrt{\delta}}{E'\sqrt{2\pi}} \tag{15}$$

As $n_j = (0, \pm 1)$ all along the crack faces, the integral of Eq. (15) contributes to J_2 only. The remaining two terms of Eq. (12) are calculated numerically, excluding the small region δ at the crack tip from the integration, now reading J_k^num [11]. An iterative procedure is necessary to calculate the analytical part J_2^ana, see Fig. 3.

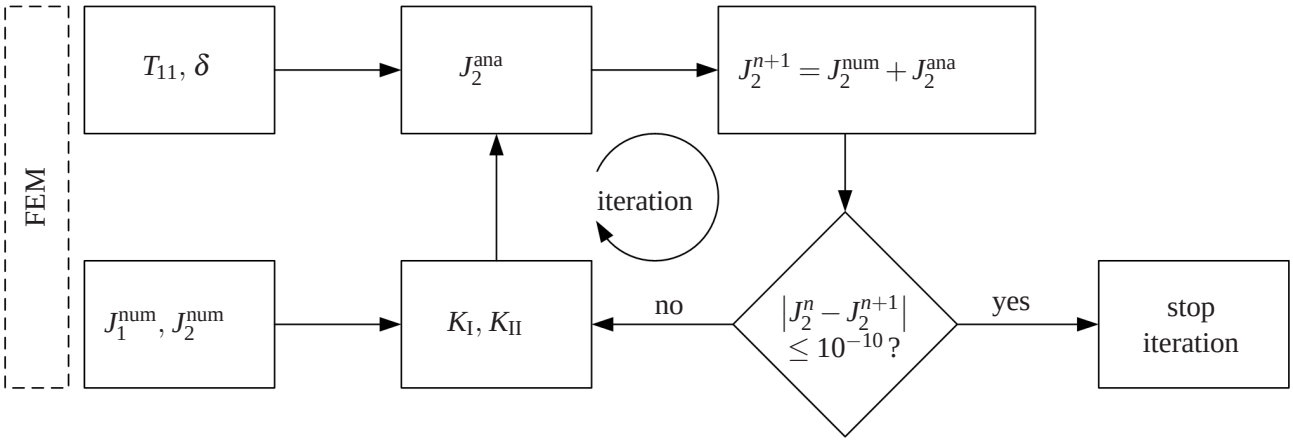

Figure 3. Flow chart of the iterative scheme for the calculation of the analytical part of the J_k-integral.

The constant T-stress on the crack faces is therefore determined at the position $r = \delta$ from the series expansion Eq. (13a):

$$T_{11} = \frac{1}{2}\left(\sigma_{11}^\mathrm{s}(\delta, +\pi) + \sigma_{11}^\mathrm{s}(\delta, -\pi)\right) \tag{16}$$

The stresses on the positive and negative crack faces $\sigma_{11}^\mathrm{s}(\delta, \pm\pi)$ are extracted from the FE calculation and substituted into Eq (16). As a first approach, K_II is calculated by substituting J_1^num and $J_2^\mathrm{num} = J_2^n$ into Eq. (11). J_2^ana is calculated by substituting T_{11}, K_II and δ into Eq. (15). The value J_2^{n+1} of the present step is the sum of J_2^num and J_2^ana. If the absolute difference between J_2^{n+1} of the present and J_2^n of the previous step is below a critical value, the iterative procedure is stopped and the final value is $J_2 = J_2^{n+1}$. If the stop criterion is not fulfilled, K_II of the next step is now calculated by substituting J_1^num and J_2^{n+1} into Eq. (11) and so on.

3.2. Method 2: Extrapolation method

The research revealed, that the incorrect calculation of J_2 is an outcome of non-symmetric numerical errors within the region δ at the crack tip, which are related to a mixed-mode loading configuration

[11]. A mixed-mode loading is a superposition of a single mode-I and single mode-II loading. Thus, the values of stresses and strains are split into parts related to mode-I and mode-II loading as follows. The stresses and displacement gradients related to the symmetric crack tip opening are calculated according to:

$$\sigma_{11}^{\mathrm{I}}(x_{\mathrm{c}}) = \frac{1}{2}\left(\sigma_{11}^{\mathrm{s}}(x_{\mathrm{c}},+\pi) + \sigma_{11}^{\mathrm{s}}(x_{\mathrm{c}},-\pi)\right) \tag{17a}$$

$$u_{1,1}^{\mathrm{I}}(x_{\mathrm{c}}) = \frac{1}{2}\left(u_{1,1}^{\mathrm{s}}(x_{\mathrm{c}},+\pi) + u_{1,1}^{\mathrm{s}}(x_{\mathrm{c}},-\pi)\right) \tag{17b}$$

The stress and displacement gradient related to the antimetric crack tip opening are determined by subtracting the symmetric parts from the total values, i.e.

$$\sigma_{11}^{\mathrm{II}}(x_{\mathrm{c}},\pm\pi) = \sigma_{11}^{\mathrm{s}}(x_{\mathrm{c}},\pm\pi) - \sigma_{11}^{\mathrm{I}}(x_{\mathrm{c}}) \tag{18a}$$

$$u_{1,1}^{\mathrm{II}}(x_{\mathrm{c}},\pm\pi) = u_{1,1}^{\mathrm{s}}(x_{\mathrm{c}},\pm\pi) - u_{1,1}^{\mathrm{I}}(x_{\mathrm{c}}) \tag{18b}$$

As the mode-I stresses and strains according to Eqs. (17) exhibit a non-singular behavior on the crack faces, extrapolating σ_{11}^{I} and $u_{1,1}^{\mathrm{I}}$ towards the crack tip is feasible. From Fig. 4(a) is becomes obvious, that particularly σ_{11}^{I} exhibits large numerical errors and thus an extrapolation is reasonable [11]. The mode-I values within $[0,\delta]$ are replaced by those, calculated from a linear regression. Rearranging Eqs. (18), the mode-I and mode-II stresses and strains are recombined and the crack face integral is calculated as usual following Eq. (9a), considering the new values. Substituting the resulting values J_k into Eq. (11), this provides accurate SIF for curved cracks under mixed-mode conditions.

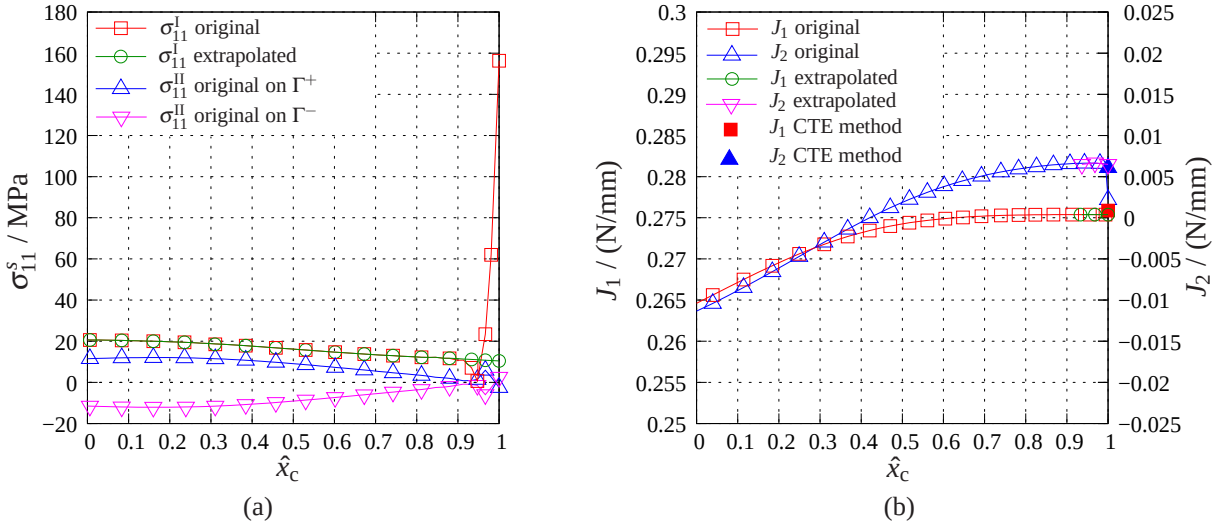

Figure 4. (a) Decomposed mode-I and mode-II stress distributions σ_{11}^{I} and $\sigma_{11}^{\mathrm{II}}$, original and extrapolated. (b) Numerically calculated J_k-integral, crack face integral calculated within the range $[0,\hat{x}_{\mathrm{c}}]$, comparison of different methods.

In Fig. 4(a) the tangential stress σ_{11}^{s} on the crack faces is plotted vs. a normalized crack face coordinate $\hat{x}_{\mathrm{c}} = (R - x_{\mathrm{c}})/R$, with $\hat{x}_{\mathrm{c}} = 1$ at the crack tip and $\hat{x}_{\mathrm{c}} = 0$ for $x_{\mathrm{c}} = R$. The considered boundary value problem is that one of a Double Cantilever Bream with dissimilar forces $F_1 = 100\mathrm{N}$ and $F_2 = 99\mathrm{N}$

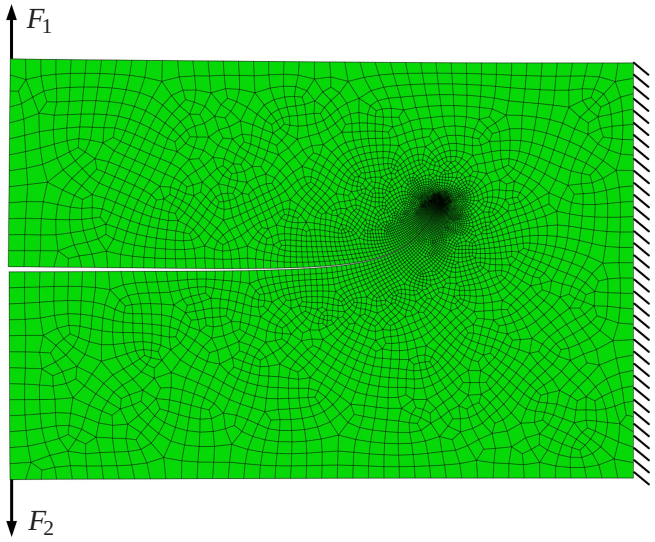

Figure 5. FE-mesh of the grown curved crack shown in a deformed configuration.

acting at the front end leading to a curved crack path, see Fig. 5. The corresponding J_k-integral calculated within the range $[0, \hat{x}_c]$ is shown in Fig. 4(b). The function $J_k(\hat{x}_c)$ has got nothing to do with path-dependence but enables to localize the incorrect contribution to the crack face integral. The value that J_k reaches approaching the crack tip $\hat{x}_1 = 1$ is the relevant loading quantity according to Eqs. (12) and (1). For the sake of comparison, results from the Crack Tip Element (CTE) method [9, 1] have been included in the figure.
The choice of the parameter δ has an influence on the results. For $\delta < \delta_c$, not all inaccurate values are excluded from the numerical integration and therefore the resulting values of J_k are inaccurate. For $\delta > \delta_c$, the values of J_k obtained by the extrapolation method (Method 2) show little influence. On the other hand, the values of J_k calculated by the analytic extension method (Method 1) show increasing deviation for increasing δ. The research revealed that the best choice of δ_c includes the region of the first three element rings around the crack tip. Both methods are suitable for the accurate calculation of the coordinate M_2^{II} as well.

Table 1. Comparison of stress intensity factors calculated from the CTE-method and the M_k-integral considering the actual crack face integral (ACFI) and the fictitious crack face integral (FCFI), neglecting FCFI only or neglecting both FCFI and ACFI.

	CTE	M_k	M_k without FCFI	M_k without FCFI and ACFI
$K_{\mathrm{I}}/(\mathrm{MPa}\sqrt{\mathrm{mm}})$	240.39	240.31	276.77	261.72
$K_{\mathrm{II}}/(\mathrm{MPa}\sqrt{\mathrm{mm}})$	-2.86	-2.95	-38.38	7.26

Results of SIF calculated from the CTE-method [9, 1] and the M_k-integral are presented in Tab. 1. It is obvious, that neglecting the integration along the fictitious crack faces of the auxiliary fields produces considerable errors. The same holds, when neglecting both the fictitious crack face integral (FCFI) and the actual crack face integral (ACFI), as shown in the last column of Tab. 1.

4. Systems of multiple interacting cracks

The loading quantities of multiple crack systems, related to every single crack tip, are calculated by path independent integrals. With regard to crack tips approaching interfaces such as material

interfaces, internal boundaries or crack surfaces, it is beneficial to evaluate the integrals along large contours containing all N tips of a multiple crack system, see Fig. 6(a). For comparison, the crack paths are simulated by calculating the integral along small contours in the vicinity of the crack tip, as shown in Fig. 6(b). The resulting value of the J_k-integral along a large contour Γ_0 equals the sum of

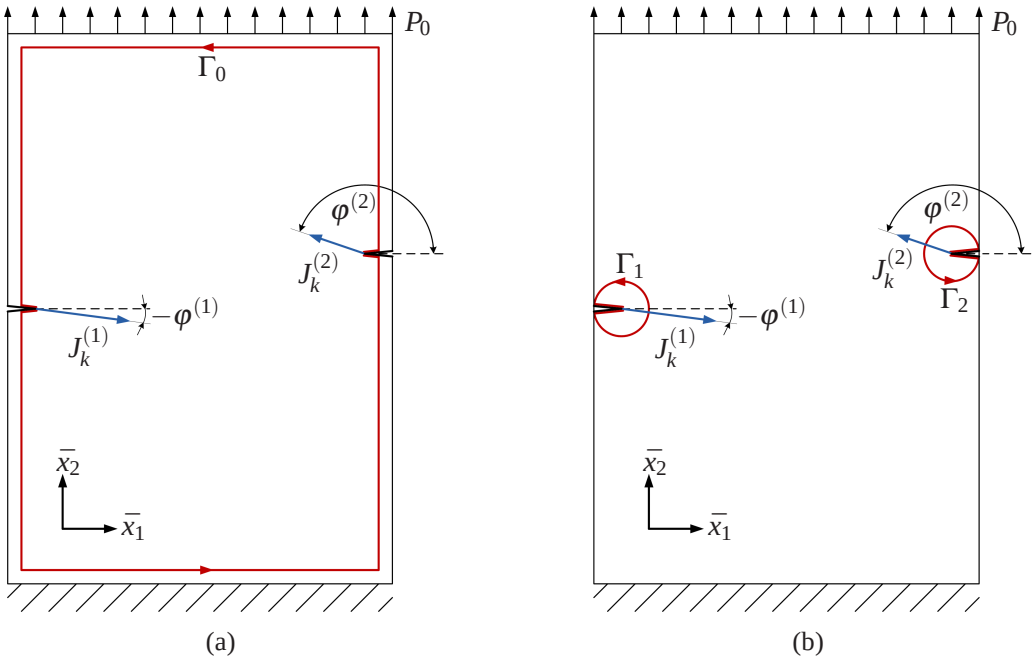

Figure 6. Integration contours Γ_0, Γ_1, Γ_2 for path-independent J_k and M_k-integral and J_k-integral vectors $J_k^{(i)}$.

the loading quantities of all N crack tips.

$$J_1 = \sum_{i=1}^{N} \cos\varphi^{(i)} \left| J_k^{(i)} \right| \tag{19a}$$

$$J_2 = \sum_{i=1}^{N} \sin\varphi^{(i)} \left| J_k^{(i)} \right| \tag{19b}$$

The angle $\varphi^{(i)}$ is related to the global coordinate system $\bar{x}_i$. The applied crack deflection criterion is that of the *maximum energy release rate*, i.e. the J_k-vector points into the direction of the crack propagation z_k, see Eq. (4). This and the principle of minimum potential energy lead to the auxiliary condition, that the sum of the absolute values of the J_k-integrals related to every single crack tip, reaches a global maximum. Further, each absolute value $J_k^{(i)}$ must be smaller or equal to the value of the critical energy release rate G_c. If another condition is required, in order to reduce the solution space it can be postulated that the crack deflection angle must be smaller or equal to a maximum value $\mathrm{d}\varphi_{\max}$. The latter criterion is motivated by the fact that cracks usually show a smooth curvature whereas sharp kinks are only observed if the loading regime is subjected to a sudden and fundamental change.

$$\sum_{i=1}^{N} \left| J_k^{(i)} \right| \stackrel{!}{=} \max \tag{20a}$$

$$\left|J_k^{(i)}\right| \leq G_c \tag{20b}$$

$$\mathrm{d}\varphi \leq \mathrm{d}\varphi_{\max} \tag{20c}$$

Developing a separation procedure to determine $J_k^{(i)}$ based on Eqs. (19), this method has to satisfy the conditions according to Eqs. (20). A numerical validation is achieved by calculating the J_k-integral along small contours around the crack tip, see Fig. 6(b). The loading quantities calculated by small contours Γ_i must be equal to the values that are calculated by the separation procedure. Here it must be taken into account that numerical errors dominate, if Γ_i is chosen too small, whereas large contours must not intersect other crack faces or boundaries. In Fig. 7(b) results of a simulation with two cracks are presented. The plate specimen is exposed to a uniform load $P_0 = 100$MPa and exhibits two non-symmetric incipient cracks of the length $a_1 = a_2 = 5$mm. All geometric dimensions are shown in Fig. 7(a). A crack growth simulation with fatigue crack growth rates assumed to be constant and equal for both cracks, leads to the crack paths as shown in Fig. 7(b).

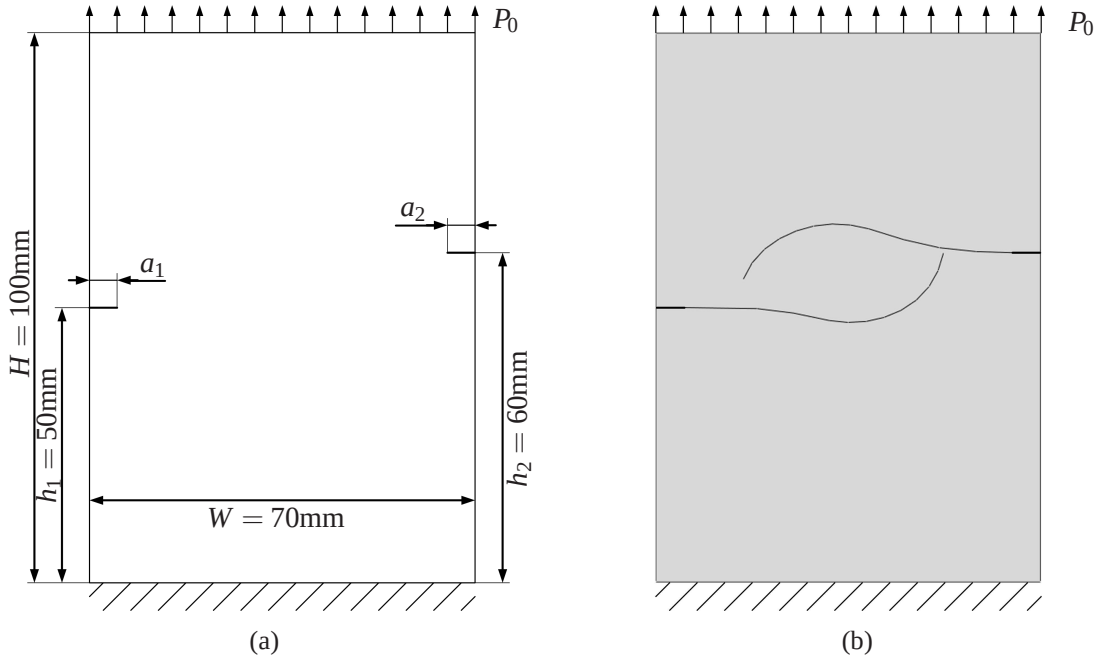

Figure 7. (a) Geometric dimensions of plate specimen exhibiting two non-symmetric incipient cracks. (b) Crack paths resulting from a crack growth simulation exposing the specimen to a uniform load $P_0 = 100$MPa.

5. Closure

Introducing path-independent integrals J_k and M_k, the necessity of the calculation of crack face integrals is outlined. Considering interfaces, internal boundaries or crack surfaces, it is beneficial to apply large contours including crack face integrals for the calculation of J_k or M_k. To achieve path-independence for the M_k-integral considering curved crack faces, an integration along the fictitious crack faces of the corresponding auxiliary fields is nessecary. When calculating the stress intensity factors or the energy release rate from path independent integrals, it is inevitable to calculate these integrals accurately. The challenging calculation of the crack face integrals is explained and two new

methods to calculate accurate values are presented. An analytical extension method and the extrapolation of singular stresses and strains on the crack faces provide very good results for straight and curved cracks.
The J_k-integral is applied to multiple crack systems, calculating a global value of J_k, being the sum of all local values related to every single crack tip. Auxiliary conditions are introduced to solve a global minimization problem. A separation procedure enables to calculate loading quantities related to each crack tip. Based on the specimen in Fig. 7, experiments are about to be carried out, in order to verify the theoretically predicted crack patterns.

References

[1] R. S. Barsoum, On the use of isoparametric finite elements in linear fracture mechanics. Int J Numer Methods Eng, 10 (1976) 25-37.

[2] D. Bergez, Determination of stress intensity factors by use of path-independent integrals. Mech Res Commun, 1 (1974) 179-180.

[3] P. O. Bouchard, F. Bay, Y. Chastel, I. Tovena, Crack propagation modelling using an advanced remeshing technique. Comput Methods Appl Mech Eng, 189 (2000) 723-742.

[4] G. P. Cherepanov, Mechanics of brittle fracture, McGraw-Hill, New York, 1979.

[5] J. W. Eischen, An improved method for computing the J_2 integral. Eng Fract Mech, 26 (1987) 691-700.

[6] J. D. Eshelby, The force on an elastic singularity. Solid State Phys, 3 (1956) 79-144.

[7] M. Gosz, J. Dolbow, B. Moran, Domain integral formulation for stress intensity factor computation along curved three-dimensional interface cracks. Int J Solids and Struct, 35 (1998) 1763-1783.

[8] M. Gosz, B. Moran, An interaction energy integral method for computation of mixed-mode stress intensity factors along non-planar crack fronts in three dimensions. Eng Fract Mech, 66 (2002) 299-319.

[9] R. D. Henshell and K. G. Shaw, Crack tip finite elements are unnecessary. Int J Numer Methods Eng, 9 (1975) 495-507.

[10] A. G. Herrmann, G. Herrmann, On energy release rates for a plane crack. J Appl Mech, 48 (1981) 525-528.

[11] P. O. Judt, A. Ricoeur, Accurate loading analyses of curved cracks under mixed-mode conditions applying the J-integral. Submitted to Int J Fract.

[12] J. R. Rice, A path independent integral and the approximate analysis of strain concentration by notches and cracks. J Appl Mech, 35 (1968) 379-386.

[13] M. Stern, E. B. Becker, R. S. Dunham, A contour integral computation of mixed-mode stress intensity factors. Int J Fract, 12 (1976) 359-368.

[14] S. S. Wang, J. F. Yau, H. T. Corten, A mixed-mode crack analysis of rectilinear anisotropic solids using conservation laws of elasticity. Int J Fract, 16 (1980) 247-259.

[15] M. L. Williams, On the stress distribution at the base of a stationary crack. J Appl Mech, 24 (1957) 109-114.

[16] G. Zi, J.-H. Song, E. Budyn, S.-H. Lee, T. Belytschko, A method for growing multiple cracks without remeshing and its application to fatigue crack growth. Model Simul Mater Sci Eng, 12 (2004) 901-915.